

Magnetic Structure of Rare-Earth Iridium Compounds $R\text{Ir}_2$

GIAN PIERO FELCHER*† AND W. C. KOEHLER
Oak Ridge National Laboratory, Oak Ridge, Tennessee
 (Received 8 April 1963)

Neutron diffraction measurements on TbIr_2 and HoIr_2 confirm the low molecular moments deduced from magnetic measurements. Partial quenching of the orbital angular momentum of the rare-earth atoms is indicated. The coherent scattering amplitude of Ir was determined to be $(1.00 \pm 0.02) \times 10^{-12}$ cm.

INTRODUCTION

THE rare-earth metals form compounds with iridium of the composition $R\text{Ir}_2$ which have the MgCu_2 type structure¹ (cubic Laves phase). Magnetic measurements on members of this series^{2,3} have shown that they are ferromagnetic with Curie points ranging from a maximum of 88°K for GdIr_2 to about 1°K for TmIr_2 . These measurements have yielded values for the molecular moments of the compounds $R\text{Ir}_2$ which are significantly lower than those expected for the ordered tripositive rare-earth ions. The low moment values may indicate the existence of a partial quenching of the orbital moment of the rare-earth ion. They may alternatively indicate the existence of a kind of ferrimagnetic structure in which the rare-earth moments are partially cancelled.

Neutron diffraction measurements have been made on specimens of two members of the series, namely, on TbIr_2 and HoIr_2 , in order to investigate the magnetic structures of these compounds. These two particular rare-earth compounds were selected because they represent the best compromise, from the experimental point of view, with respect to expected moment value, absorption cross section, and Curie temperature.

SAMPLE PROPERTIES AND PROCEDURE

The samples were prepared by the arc melting of stoichiometric proportions of the pure metals. The resulting brittle buttons were crushed to pass through an 80-mesh sieve, and the powder was loaded into a specially designed flat diffraction cell. A very thin cell of large cross section was used to optimize the scattering from the highly absorbing sample (the capture cross section for iridium at thermal energy is 430 b). Room-temperature x-ray diffraction patterns showed lines characteristic of the cubic Laves phase only, and the patterns yielded lattice parameters of 7.524 and 7.503 Å, respectively, for TbIr_2 and HoIr_2 . Neutron diffraction patterns were obtained at room temperature, at 77°K, and at temperatures near that of liquid helium. Limited angular regions in the diffraction patterns were

studied at intermediate temperatures in order to establish the transition temperatures.

The unit cell of the $R\text{Ir}_2$ structure contains eight molecules with the rare-earth atoms in the special positions $(000, \frac{1}{4}, \frac{1}{4}, \frac{1}{4} + \text{F.C.})$ of the space group $F_{d3m} - O_h^7$. The rare-earth atom distribution is identical to that of the carbon atoms in the diamond structure. There are sixteen iridium atoms in the structure which can be envisaged as forming four tetrahedra, the centers of which are located at $(\frac{3}{4}, \frac{3}{4}, \frac{3}{4} + \text{F.C.})$. As a result of the high symmetry of this structure there are many systematic absences in the powder patterns. Moreover, the intensities of some reflections, (220), (620), etc., are due to scattering by rare-earth atoms alone, and of others (222), (622), etc., to that from iridium atoms alone. This property has proved to be of importance in the analysis of the magnetic scattering data.

RESULTS AND DISCUSSION

The room-temperature neutron-diffraction data for TbIr_2 and HoIr_2 were analyzed in the usual way by a comparison of the scattering with that from a standard sample. From the absolute intensities in the TbIr_2 pattern, the following scattering amplitudes were deduced: $b_{\text{Tb}} = (0.76 \pm 0.02) \times 10^{-12}$ cm, $b_{\text{Ir}} = (1.01 \pm 0.02) \times 10^{-12}$ cm. This value of the terbium amplitude agrees well with that determined in other measurements.³ The iridium amplitude is in accord with the value $b_{\text{Ir}} = (0.99 \pm 0.015) \times 10^{-12}$ cm which was independently measured during the course of this study from pure iridium powder.⁴

A summary of observed and calculated nuclear intensities for TbIr_2 is given in the first columns of Table I. The intensity agreement is excellent except for the very weakest reflections and is considered to be satisfactory. Similar results were obtained from the pattern of HoIr_2 .

At very low temperatures the diffraction patterns of both compounds show evidence for the development of long-range magnetic order. There is a marked reduction in the background scattering, and there are observed magnetic contributions to many of the coherent reflections. No additional reflections, however, are observed. The diffraction patterns are, therefore,

⁴ This value for b_{Ir} is very much higher than that reported in the literature [S. S. Sidhu, LeRoy Heaton, and M. H. Mueller, *Progr. Nucl. Energy, Ser. V*, **3**, 419 (1961)]. The Argonne data have recently been reinterpreted to yield a value of b_{Ir} which is close to the value cited in the text. [M. H. Mueller (private communication).]

* International Atomic Energy Commission Fellow.

† Present address: Comitato Nazionale per l'Energia Nucleare, Centro di Studi Nucleari della Casaccia, Rome, Italy.

¹ V. B. Compton and B. T. Matthias, *Acta Cryst.* **12**, 651 (1959).

² R. M. Bozorth, B. T. Matthias, H. Suhl, E. Corenzwit, and D. D. Davis, *Phys. Rev.* **115**, 1595 (1959).

³ Unpublished ORNL data; see also M. Atoji, *J. Chem. Phys.* **35**, 1950 (1961).

typical of those from ferromagnetic or ferrimagnetic structures. The relative magnitudes of the nuclear and magnetic contributions to the observed reflections in TbIr_2 are illustrated by the entries in column 4 of Table I.

If one assumes that the iridium atoms carry no magnetic moment, the magnetic intensities can be reduced to values of $(\mu f)^2$, where μ is the magnitude of the ordered rare-earth moment in the ferromagnetic structure and f is the rare-earth form factor. The results of this reduction for the data of TbIr_2 are summarized in Fig. 1 where values of $(\mu f)^2$ derived from the coherent magnetic reflections are indicated by open circles. It may be emphasized that the value of $(\mu f)^2$ for (220) is independent of the assumption made above, since the intensity of this reflection has no contribution from iridium. For reflections which occur at higher values of $(\sin\theta)/\lambda$; e.g., $(\sin\theta)/\lambda > 0.2$, the contribution made by any reasonable Ir moment is negligible. This follows as a result of the very rapid fall off with $(\sin\theta)/\lambda$ of the Pauling-Sherman form factor for iridium. With the possible exception of the reflection (111) then, the magnetic intensities in the coherent reflections can be converted, with the knowledge of the form factor, to a value for the ordered moment per Tb atom. With the form factor deduced from measurements on⁵ TbN the data yield an ordered moment of $7.48 \pm 0.20 \mu_B$ for Tb in TbIr_2 .

The solid curve in Fig. 1 was computed from the above value of the moment and from the TbN form factor. It is noteworthy that the point for (111) lies on the curve.

The magnetic intensities listed in the last column of Table I were calculated on the ferromagnetic model in which each Tb atom has the moment and form factor described above. For a polycrystalline specimen of such a structure the moment directions are indeterminate

TABLE I. Comparison of nuclear intensities observed at room temperature and nuclear and magnetic intensities at 4.2°K for TbIr_2 . Intensities are expressed in units of thousands of counts. For the magnetic intensity calculations an ordered moment of $7.5 \mu_B$ for Tb is used. No moment is assumed for Ir.

Index	$I_n(\text{obs})$	$I_n(\text{calc})$	$I_{n+m}(\text{obs})$	$I_{n+m}(\text{calc})$
111	5.87	5.74	41.2	41.4
200	0	0	0	0
220	8.31	8.18	38.7	39.5
311	71.7	74.2	93.4	95.8
222				
400	6.36	5.24	12.4	12.6
331	3.02	2.46	11.7	12.6
420	0	0	0	0
422	5.02	4.99	15.4	14.6
511				
333	24.7	23.9	30.7	31.3
440	23.2	23.6	27.6	28.1

⁵ H. R. Child, M. K. Wilkinson, E. O. Wollan, J. W. Cable, and W. C. Koehler, Phys. Rev. **131**, 922 (1963).

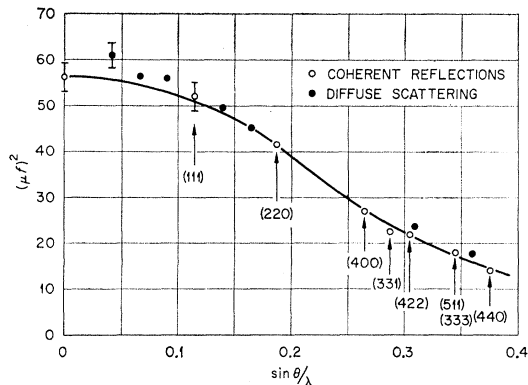


FIG. 1. Variation with $(\sin\theta)/\lambda$ of $(\mu f)^2$ for TbIr_2 . Open circles represent data from indicated coherent magnetic reflections. Closed circles are data derived from the diffuse scattering. The solid curve is calculated from the Tb form factor and a moment of $7.48 \mu_B$ for Tb.

and the average value of $\frac{2}{3}$ for the square of the magnetic interaction vector, q^2 , is appropriate to all reflections. The agreement between calculated and observed intensities at low temperatures is quite satisfactory.

An independent measurement of the ordered moment was obtained from an analysis of the difference diffuse scattering, e.g., from the difference in diffuse scattering at temperatures well above and well below the ordering temperature. The results of this analysis are shown by the closed circles of Fig. 1. These data extrapolate to a slightly higher value for the ordered moment, $7.74 \pm 0.20 \mu_B$, which is, however, well within experimental error of the value obtained from the coherent reflections.

The Curie points for TbIr_2 and HoIr_2 were determined from the measured variation with temperature of the intensity in the (111) reflection. The values obtained, (46 ± 1) and $(13 \pm 1)^\circ\text{K}$ agree quite well with the corresponding values reported by Bozorth *et al.*²

Because of the low Curie point for HoIr_2 the magnetic intensities in its diffraction pattern are not completely developed at the lowest temperature studied. Nevertheless, an analysis of the data can be made in a manner analogous to that already described for TbIr_2 , and that analysis leads to a value for the moment of Ho at 8.0°K of $6.5 \mu_B$. Extrapolation of the temperature-intensity curve of the (111) reflection yields a value of 7.2 ± 0.3 for the ordered moment of Ho in HoIr_2 .

The molecular moments for TbIr_2 and HoIr_2 measured by Bozorth *et al.*, 7.0 and $7.5 \mu_B$ are much smaller than the values expected for ordered tripositive rare earth ions: $9.0 \mu_B$, Tb, $10.0 \mu_B$, Ho. Since the moments measured from the neutron diffraction data for the rare-earth atoms themselves have values less than gJ , it must be concluded that the orbital moments of the rare-earth atoms are partially quenched.

It remains to ask if the difference between $7.0 \mu_B$ for TbIr_2 and $7.5 \mu_B$ for Tb in TbIr_2 may be significant.

The precision of the neutron measurements is such that a small moment on iridium, 0.2–0.3 μ_B , would just be detectable. However, it is known^{2,6} that there exists a range of compositions for these and similar compounds over which the Laves phase structure is found. If a 3% weight loss on melting, as noted by Bozorth and co-workers, be attributed to loss of Tb then one would have

⁶ J. H. Wernick and S. Geller, *Trans. AIME* **218**, 866 (1960).

to do with $\text{Tb}_{0.9}\text{Ir}_2$ ⁷ rather than TbIr_2 and a moment differing by some 10% from that of the ideal compound would be inferred. It appears impossible to us to state at this time that iridium does or does not carry a small magnetic moment.

⁷ Direct chemical analysis of the TbIr_2 specimen investigated here gives a composition $\text{Tb}_{1.01}\text{Ir}_2$, which is not distinguishable, in our measurement, from the ideal composition. A change from the ideal composition of 10% Tb would, however, create fluctuations in the nuclear intensity which would be easily detectable.

Galvanomagnetic Phenomena in High Electric Fields

HERBERT F. BUDD

Laboratoire de Physique de l'École Normale Supérieure, Paris, France

(Received 31 December 1962; revised manuscript received 2 May 1963)

The Hall coefficient in a many-valley semiconductor is calculated for high electric fields and is shown to be independent of the electric field. For silicon we find $R_{100}/R_{111}=0.9$ and $R_{110}/R_{111}=0.85$, where R_{100} is the Hall coefficient for the current in the [100] direction, etc. For germanium we find $R_{111}/R_{100}=0.68$. Distribution functions for hot electrons in high magnetic fields are calculated at high and low temperatures for acoustical phonon scattering.

IN this paper we shall consider the galvanomagnetic properties of a system of electrons in a strong electric field. Sodha and Eastman¹ have calculated the electric-field dependence of the low-magnetic-field Hall coefficient for the case of a simple parabolic energy band and scattering by acoustical phonons.

Conwell² has used McClure's³ solution of the Boltzmann equation to obtain general expressions for the Hall coefficient in a many-valley semiconductor in terms of the electron-distribution function. The conditions under which one may use McClure's treatment to describe a system of hot electrons have been discussed qualitatively by Conwell.

In this treatment we separate the general Boltzmann equation for a many-valley semiconductor into coupled equations for the isotropic and anisotropic parts of the distribution function. The equation for the anisotropic part is shown to be identical with McClure's equation except for an additional term which is shown to be negligible. The equation for the isotropic part allows one to calculate the electric and magnetic field dependence of the distribution function for arbitrary fields.

In Sec. II, we calculate the low-magnetic-field Hall coefficient using the hot-electron distribution obtained by Reik and Riskin.⁴ Results are obtained for several current directions in silicon and germanium. In Sec. III we calculate the distribution function for hot electrons in high magnetic fields for acoustical phonon scattering.

¹ M. S. Sodha and P. C. Eastman, *Phys. Rev.* **110**, 1314 (1958).

² E. M. Conwell, *Phys. Rev.* **123**, 454 (1961).

³ J. W. McClure, *Phys. Rev.* **101**, 1642 (1956).

⁴ H. G. Reik and H. Riskin, *Phys. Rev.* **124**, 777 (1961).

I. THE BOLTZMANN EQUATION

The time-independent Boltzmann equation is given by

$$e(\mathbf{E} + \mathbf{V} \times \mathbf{B}) \cdot \nabla_{\mathbf{K}} f = \hat{C} f, \quad (1)$$

where \mathbf{E} and \mathbf{B} are the electric and magnetic fields, \hat{C} is the collision operator, and \mathbf{K} and \mathbf{V} are the wave vector and velocity, respectively. We consider a many-valley semiconductor with ellipsoidal constant energy surfaces. In the coordinate system of the principal axes of the valley under consideration, the electron energy is given by

$$\epsilon = K_x^2/2m_x + K_y^2/2m_y + K_z^2/2m_z. \quad (2)$$

Transforming these ellipsoidal surfaces into spheres, Eqs. (1) and (2) become

$$e(\mathbf{E}' + \mathbf{V}' \times \mathbf{B}') \cdot \nabla_{\mathbf{K}'} f = \hat{C}' f; \quad \epsilon = \mathbf{K}'^2/2m_0,$$

where

$$\begin{aligned} \mathbf{K}' &= \alpha \mathbf{K}, & \mathbf{B}' &= R \mathbf{B}, & \mathbf{E}' &= \alpha \mathbf{E}, & \mathbf{V}' &= \mathbf{K}'/m_0, \\ \alpha &= \begin{bmatrix} m_0/m_x & 0 & 0 \\ 0 & m_0/m_y & 0 \\ 0 & 0 & m_0/m_z \end{bmatrix}^{1/2}, \\ R &= \begin{bmatrix} m_x & 0 & 0 \\ 0 & m_y & 0 \\ 0 & 0 & m_z \end{bmatrix}^{1/2} \frac{m_0}{(m_x m_y m_z)^{1/2}}. \end{aligned} \quad (3)$$

We now separate f into two parts S and A : $f = S + A$,